PHYSICAL REVIEW D **79,** 014017 (2009)

Refined analysis of photon leptoproduction off a spinless target

A. V. Belitsky[1] and D. Müller[2]

[1]*Department of Physics, Arizona State University, Tempe, Arizona 85287-1504, USA*
[2]*Institut für Theoretische Physik II, Ruhr-Universitat Bochum, D-44780 Bochum, Germany*

(Received 5 November 2008; published 20 January 2009)

We calculate the differential cross section for real-photon electroproduction off a spinless hadron which serves as a main probe of the hadrons structure via the concept of generalized parton distributions. Compared to previously available computations performed with twist-three power accuracy, we exactly accounted for all kinematical effects in hadron mass and momentum transfer which arise from leptonic helicity amplitudes. We performed numerical studies of these kinematical effects and demonstrated that in the valence quark region and rather low virtualities of the hard photon which sets the factorization scale, the available approximate results significantly overestimate the cross section rates in comparison to exact formulas.

DOI: 10.1103/PhysRevD.79.014017 PACS numbers: 13.60.−r, 12.38.Bx

I. INTRODUCTION

The qualitative mechanism which binds hadronic constituents together in a bound state is well understood within the framework of QCD via the formation of collimated gluon flux tubes between quarks. This picture is confirmed by lattice gauge theory simulations which aim at a quantitative exploration of the hadronic structure. However, physical observables which can be measured in high-energy experiments necessarily involve correlation functions of elementary quark and gluon fields separated by lightlike distances and thus evade straightforward use of Euclidean lattice tools. Therefore, in the lack of other analytical/numerical first-principle techniques, phenomenological analyses of experimental data are currently the only viable alternative route to unravel manifestations of the intricate bound state problem in QCD.

Among hadronic observables, generalized parton distributions (GPDs) [1] are the most elaborate light-cone correlation functions containing simultaneous information on both position and momentum distributions of strongly interacting constituents [2,3]. Similarly to conventional collinear parton densities which are measured in deeply inelastic scattering, GPDs can be probed in experiments involving electroweak bosons with production of a real photon or mesons in the final state (see Ref. [4] for reviews). While the meson production receives contamination from additional hadronic final states, the former are free from these uncertainties and provide a clean access to hadronic inner content through GPDs.

To date, the most complete analytic calculations were performed for the photon leptoproduction cross section off spin-zero and spin-one-half targets and were limited to twist-three accuracy. This approximation implies that only terms suppressed by a single power of the hard photon virtuality were kept in all analytical expressions, corresponding both to leptonic and hadronic parts of amplitudes. The latter is defined by the expectation value of the chronological product of two electromagnetic currents between in and out hadronic states,

$$T_{\mu\nu} = i \int d^4 z \mathrm{e}^{(i/2)(q_1+q_2)\cdot z} \langle p_2 | T\{ j_\mu(z/2) j_\nu(-z/2)\} | p_1 \rangle. \tag{1.1}$$

This tensor is parametrized in terms of the so-called Compton form factors (CFFs) $\mathcal{F}(\xi, t; \mathcal{Q})$ which enter as coefficients in front of independent Lorentz structures. The CFFs depend on the generalized Bjorken-like scaling variable ξ, the squared momentum transfer t, and the photon virtuality $q_1^2 = -\mathcal{Q}^2$. The QCD factorization theorems are indispensable in separating CFFs in terms of short-distance coefficient functions $C(x, \xi; \mathcal{Q}/\mu)$, controllable via conventional perturbation theory in the QCD coupling constant, and long-distance dynamics encoded in GPDs $F(x, \xi, t; \mu)$,

$$\mathcal{F}(\xi, t; \mathcal{Q}) = \int dx C(x, \xi; \mathcal{Q}/\mu) F(x, \xi, t; \mu). \tag{1.2}$$

The state-of-the-art considerations of the hadronic tensor (1.1) were done in the twist-three approximation [5–9]. The hierarchy of hadronic matrix elements of higher-twist operators emerging in the operator product expansion of Eq. (1.1) suggests smallness of their effect on event rates even at rather low virtualities. This phenomenon is well known in deeply inelastic scattering and yields precocious scaling of corresponding observables making the neglect of operators of twist-four and higher legitimate. On the other hand, the approximation to merely leading and first subleading contributions stemming from the leptonic tensor were an artifact of matching the expansion of hadronic and leptonic parts. When the latter approximation is waived, numerical considerations demonstrate significant deviations between the two predictions for the kinematics of Jefferson Lab experiments. Therefore, in the present paper we perform a refined analysis starting with leptoproduction cross section of real photons off a spinless target. The result

is from phenomenological interest for deeply virtual Compton scattering off spin-zero nuclei and it improves formulae for cross section and asymmetries [10,11]. In our numerical examples we will, however, equate the target mass with the nucleon one to illuminate the size of corrections, expected for the deeply virtual Compton scattering (DVCS) off an unpolarized proton.

Our subsequent consideration is organized as follows. In the next section, we present a brief profile of the twist-three formalism we have developed in our earlier work [10]. In Sec. IV, we introduce the formalism of helicity amplitudes [12,13] which proves to be very efficient in separating power-suppressed effects arising from strong-coupling dynamics in the form of higher-twist correlations, on the one hand, and kinematical effects due to nonvanishing masses of hadrons and momentum transfer in the t-channel, on the other. As previously, the hadronic part is calculated to twist-three accuracy, while we account for aforementioned kinematically suppressed contributions exactly and thus keep all power effects in the leptonic part. As a consequence, the very transparent classification scheme of Ref. [10], which allows one to identify Fourier harmonics in the azimuthal angle with specific twists of contributing GPDs, ceases its existence at small photon virtuality in the valence region. Then in Sec. IV C and V, we provide an estimate of different contributions to the cross section to get a handle on the most sizable effects. Finally, we conclude. The discussion of the kinematics is deferred to Appendix A, while the explicit expressions for leptonic helicity amplitudes are summarized in Appendix B.

II. ELECTROPRODUCTION CROSS SECTION

The main focus of our present analysis is the fourfold cross section for the scattering of a light lepton $\ell = e^{\mp}$ off a spinless hadron h and production of a photon in the final state, $\ell(k)h(p_1) \to \ell(k')h(p_2)\gamma(q_2)$,

$$d\sigma = \frac{\alpha^3 x_{\rm B} y}{8\pi \mathcal{Q}^2\sqrt{1+\epsilon^2}} \left|\frac{\mathcal{T}}{e^3}\right|^2 dx_{\rm B}\, dy\, d|t|\, d\phi. \tag{2.1}$$

The phase space of the process is parametrized by the Bjorken variable $x_{\rm B} = \mathcal{Q}^2/(2p_1\cdot q_1)$ defined by the virtual photon Euclidean mass $\mathcal{Q}^2 = -q_1^2$ of momentum $q_1 = k - k'$, the squared momentum transfer $t \equiv \Delta^2$ with $\Delta = p_2 - p_1$, the lepton energy loss $y = p_1\cdot q_1/p_1\cdot k$, and finally the azimuthal angle ϕ of the outgoing hadron. The dependence on the latter provides a very important handle on different combinations of twist-two and twist-three GPDs which enter the hadronic amplitudes (1.1). The cross section depends on small kinematical parameters which we will account for exactly in the present consideration. One of them has already appeared explicitly in Eq. (2.1) and is given by the ratio of the hadronic mass M to the photon virtuality $\mathcal{Q}$,

$$\epsilon \equiv 2x_{\rm B}\frac{M}{\mathcal{Q}}. \tag{2.2}$$

The other will be introduced below.

According to Fig. 1, the amplitude of the process $\mathcal{T}$ is a sum of two distinct contributions, one involving the DVCS tensor (1.1) and termed $\mathcal{T}^{\rm DVCS}$ and the other one with leptonic Bethe-Heitler (BH) subprocess coupled to the hadronic electromagnetic current J_μ parametrized via the (pseudo)scalar form factor $F(t)$ as

$$J_\mu = \langle p_2|j_\mu(0)|p_1\rangle = (p_1+p_2)_\mu F(t), \tag{2.3}$$

and dubbed $\mathcal{T}^{\rm BH}$. The latter is real (to the lowest order in the QED fine structure constant) and $F(t)$ is taken from other measurements. The azimuthal angular dependence of each of the three terms in

$$\mathcal{T}^{\,2} = |\mathcal{T}^{\rm BH}|^2 + |\mathcal{T}^{\rm DVCS}|^2 + \mathcal{I}, \tag{2.4}$$

with the interference term

$$\mathcal{I} = \mathcal{T}^{\rm DVCS}(\mathcal{T}^{\rm BH})^* + (\mathcal{T}^{\rm DVCS})^*\mathcal{T}^{\rm BH}, \tag{2.5}$$

arises from the Lorentz-invariant scalar products defining the leptonic and hadronic parts of amplitudes as explained at length below. Since the square of the Bethe-Heitler amplitude was computed exactly in Ref. [14], we will focus our attention on the remaining contributions. Both of them are expressed by contractions of leptonic tensors with corresponding hadronic transition amplitudes, involving either the square of the DVCS amplitudes for $|\mathcal{T}^{\rm DVCS}|^2$, or being linear both in the DVCS and hadronic electromagnetic current for $\mathcal{I}$,

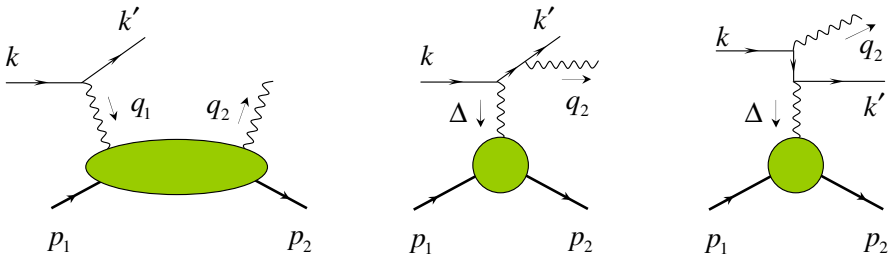

FIG. 1 (color online). Amplitudes contributing to the photon leptoproduction cross section. The first one (i.e., the leftmost) is the DVCS amplitude factorized into GPDs while the other two are the Bethe-Heitler amplitudes parametrized by hadronic electromagnetic form factors.

$$|\mathcal{T}^{\mathrm{DVCS}}|^2 = -\frac{e^6}{\mathcal{Q}^2} L^{\mu\nu}(\lambda) T_{\tau\mu} (T^{\tau}{}_{\nu})^*, \tag{2.6}$$

$$\mathcal{I} = \frac{\pm e^6}{\Delta^2 \mathcal{P}_1(\phi)\mathcal{P}_2(\phi)} \{ L_{\mu\nu\tau}(\lambda) T^{\tau\mu} (J^{\nu})^* + L^*_{\mu\nu\tau}(\lambda) (T^{\tau\mu})^* J^{\nu} \}. \tag{2.7}$$

Here the $+$ ($-$) sign in the interference stands for the negatively (positively) charged lepton beam. The leptonic tensors to the lowest order in the fine structure constant read,[1] respectively,

$$L_{\mu\nu}(\lambda) = \frac{2}{\mathcal{Q}^2} (k_\mu k'_\nu + k_\nu k'_\mu - k \cdot k' g_{\mu\nu} + i\lambda \varepsilon_{\mu\nu kk'}), \tag{2.8}$$

$$L_{\mu\nu\tau}(\lambda) = \frac{(k-q_2)^2 (k-\Delta)^2}{\mathcal{Q}^6} \,\mathrm{tr}\, \frac{1}{2}(1-\lambda\gamma_5) \times \{ \gamma_\nu (\not{k} - \not{\Delta})^{-1} \gamma_\tau + \gamma_\tau (\not{k}' + \not{\Delta})^{-1} \gamma_\nu \not{k}' \} \gamma_\mu \not{k}, \tag{2.9}$$

where the lepton mass has been set to zero. The rescaled BH propagators

$$\mathcal{P}_1 \equiv \frac{(k-q_2)^2}{\mathcal{Q}^2} = 1 + \frac{2k\cdot\Delta}{\mathcal{Q}^2}, \qquad \mathcal{P}_2 \equiv \frac{(k-\Delta)^2}{\mathcal{Q}^2} = \frac{t - 2k\cdot\Delta}{\mathcal{Q}^2}, \tag{2.10}$$

emerge as contaminating sources of the azimuthal angle dependence which interfere with Fourier harmonics accompanying the generalized Compton form factors if expanded in inverse powers of the large photon virtuality $\mathcal{Q}^2$. Thus they will be treated exactly.

To continue our discussion we choose the target rest frame as shown in Fig. 2. The explicit components of particle's momenta in this frame are defined in Appendix A. Guarded with these, one immediately computes all invariant products in terms of variables of the phase space of the process. For instance, one finds for the angular dependence of the BH propagators,

$$k\cdot\Delta = -\frac{\mathcal{Q}^2}{2y(1+\epsilon^2)} \left\{ 1 + 2K\cos\phi - \frac{t}{\mathcal{Q}^2} \left(1 - x_{\mathrm{B}}(2-y) + \frac{y\epsilon^2}{2} \right) + \frac{y\epsilon^2}{2} \right\}, \tag{2.11}$$

where the $1/\mathcal{Q}$-power-suppressed kinematical K factor, also showing up below in the Fourier expansion (3.1) and (3.2), reads

[1]We adopt the conventions for Dirac matrices and Lorentz tensors from Itzykson and Zuber [15], e.g., $\varepsilon^{0123} = +1$. We assume that the lepton helicity is positive, i.e., $\lambda = +1$ if the spin is aligned with the direction of the lepton three-momentum.

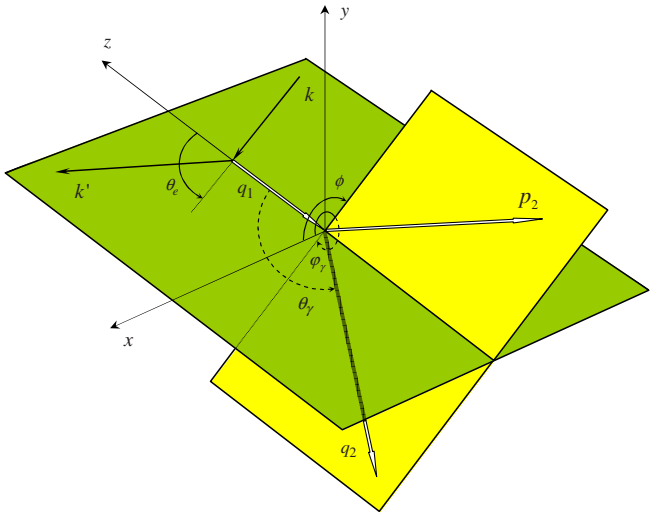

FIG. 2 (color online). The kinematics of the leptoproduction in the target rest frame. The z direction is chosen counter-along the three-momentum of the incoming virtual photon. The lepton three-momenta form the lepton scattering plane, while the recoiled proton and outgoing real photon define the hadronic scattering plane. In this reference system the azimuthal angle of the scattered lepton vanishes, while the azimuthal angle between the lepton plane and the recoiled proton momentum is ϕ.

$$K^2 = -\frac{t'}{\mathcal{Q}^2}(1-x_{\mathrm{B}}) \left(1 - y - \frac{y^2\epsilon^2}{4} \right) \left\{ \sqrt{1+\epsilon^2} + \frac{4x_{\mathrm{B}}(1-x_{\mathrm{B}}) + \epsilon^2}{4(1-x_{\mathrm{B}})} \frac{t'}{\mathcal{Q}^2} \right\}, \tag{2.12}$$

with the plus sign taken for the square root in Eq. (2.11) and the variable t' standing for

$$t' = t - t_{\mathrm{min}}. \tag{2.13}$$

The variable K vanishes at the kinematical boundary $t = t_{\mathrm{min}}$, determined by the minimal value of the momentum transfer in t channel

$$t_{\mathrm{min}} = -\mathcal{Q}^2 \frac{2(1-x_{\mathrm{B}})(1-\sqrt{1+\epsilon^2}) + \epsilon^2}{4x_{\mathrm{B}}(1-x_{\mathrm{B}}) + \epsilon^2}, \tag{2.14}$$

as well as at maximal value of the lepton energy loss $y_{\mathrm{max}} = 2\epsilon^{-2}(\sqrt{1+\epsilon^2} - 1)$.

III. BKM APPROXIMATION

In the frame we have chosen for our analysis, the contractions between the leptonic and hadronic tensor structures yield finite sums of Fourier harmonics, whose maximal frequencies are defined by the rank-m of the leptonic tensor in the incoming lepton momentum k_μ. Note, however, that the polarization-dependent part of the leptonic tensors possesses one power of the four-vector k_μ less than in the unpolarized sector. As a consequence,

the highest harmonic accompanied by the lepton helicity λ will be $\sin([m-1]\phi)$ rather than $\sin(m\phi)$, such that one finds for squared amplitudes

$$|\mathcal{T}^{\rm DVCS}|^2 = \frac{e^6}{y^2\mathcal{Q}^2}\Big\{c_0^{\rm DVCS} + \sum_{n=1}^{2}[c_n^{\rm DVCS}\cos(n\phi) + s_n^{\rm DVCS}\sin(n\phi)]\Big\}, \tag{3.1}$$

$$\mathcal{I} = \frac{\pm e^6}{x_{\rm B}y^3 t\mathcal{P}_1(\phi)\mathcal{P}_2(\phi)}\Big\{c_0^{\mathcal{I}} + \sum_{n=1}^{3}[c_n^{\mathcal{I}}\cos(n\phi) + s_n^{\mathcal{I}}\sin(n\phi)]\Big\}. \tag{3.2}$$

The generation of new harmonics in the azimuthal angle terminates at the twist-three level. The leading term (in inverse powers of the hard scale $\mathcal{Q}$) in each Fourier coefficient[2] was computed in Ref. [14] and will be presented below for the sake of comparison with improved approximations computed in the next section. Here we will point out that the leading contributions to $c_1^{\mathcal{I}}$, $s_1^{\mathcal{I}}$ as well as $c_0^{\rm DVCS}$ emerge from twist-two GPDs [13,16]. The rest of the Fourier harmonics provides an additional angular dependence and is given in terms of twist-two, i.e., for $c_0^{\mathcal{I}}$, and twist-three GPDs, i.e., for $c_1^{\rm DVCS}$, $s_1^{\rm DVCS}$, $c_2^{\mathcal{I}}$, and $s_2^{\mathcal{I}}$. The harmonics proportional to $\cos(3\phi)$ [$\cos(2\phi)$] or $\sin(3\phi)$ [$\sin(2\phi)$] in the interference [squared DVCS] term stem from the twist-two double helicity-flip gluonic GPDs alone. They are not contaminated by any twist-two quark amplitudes, however, will be affected by twist-four power corrections [17]. We neglect in our consequent considerations the effects of dynamical higher-twist (larger than three) contributions by the token alluded to in the introduction.

A. Squared DVCS amplitude

The Fourier coefficients of $|\mathcal{T}^{\rm DVCS}|^2$ naturally split into the product of factors depending on the leptonic kinematical variables and hadronic functions $\mathcal{C}^{\rm DVCS}$

$$c_0^{\rm DVCS} = 2(2-2y+y^2)\mathcal{C}^{\rm DVCS}(\mathcal{H},\mathcal{H}^*;\mathcal{H}_T,\mathcal{H}_T^*), \tag{3.3}$$

$$\begin{Bmatrix} c_1^{\rm DVCS} \\ s_1^{\rm DVCS}\end{Bmatrix} = \frac{8K}{2-x_{\rm B}}\begin{Bmatrix}(2-y)\Re{\rm e} \\ -\lambda y\Im{\rm m}\end{Bmatrix}\mathcal{C}^{\rm DVCS}(\mathcal{H}^{\rm eff};\mathcal{H}^*;\mathcal{H}_T^*), \tag{3.4}$$

$$c_2^{\rm DVCS} = \frac{16\mathcal{Q}^2K^2}{M^2(2-x_{\rm B})^2}\Re{\rm e}\mathcal{C}_T^{\rm DVCS}(\mathcal{H},\mathcal{H}_T^*). \tag{3.5}$$

The latter are bilinear in the CFFs and, respectively, read

$$\mathcal{C}^{\rm DVCS}(\mathcal{H},\mathcal{H}^*,\mathcal{H}_T,\mathcal{H}_T^*) = \mathcal{H}\mathcal{H}^* + \frac{\tilde{K}^4}{(2-x_{\rm B})^4}\mathcal{H}_T\mathcal{H}_T^*,$$
$$\mathcal{C}^{\rm DVCS}(\mathcal{H}_{\rm eff};\mathcal{H}^*;\mathcal{H}_T^*) = \mathcal{H}_{\rm eff}\Big(\mathcal{H}^* + \frac{2\tilde{K}^2}{M^2(2-x_{\rm B})^2}\times\mathcal{H}_T^*\Big)$$
$$\mathcal{C}_T^{\rm DVCS}(\mathcal{H},\mathcal{H}_T^*) = \mathcal{H}\mathcal{H}_T^*. \tag{3.6}$$

At this point, we would like to recall that the spinless hadron acquires only two types of leading twist GPDs, unpolarized quark GPD H and gluon transversity GPD H_T giving corresponding names to the CFFs (1.2). In the adopted approximation, the $c_0^{\rm DVCS}$ harmonic is expressed via the twist-two CFF $\mathcal{H}$, while the coefficients $c_1^{\rm DVCS}$ and $s_1^{\rm DVCS}$ arise from the interference of twist-two and effective twist-three CFFs,

$$\mathcal{H}^{\rm eff} \equiv -2\xi\Big(\frac{1}{1+\xi}\mathcal{H} + \mathcal{H}^3\Big),$$
$$\mathcal{H}^3 = \mathcal{H}_+^3 - \mathcal{H}_-^3, \tag{3.7}$$

with the CFFs $\mathcal{H}_\pm^3$ related to functions $H_\pm^3$ given by a convolution of the twist-two GPD H and the so-called Wandzura-Wilczek kernel provided one neglects dynamical quark-gluon-quark correlation functions [14]. Here the generalized Bjorken variable ξ is related to the usual one $x_{\rm B}$ via $\xi \simeq x_{\rm B}/(2-x_{\rm B})$. Finally, the Fourier coefficients $c_2^{\rm DVCS}$ and $s_2^{\rm DVCS}$ are induced by the gluon transversity CFFs.[3]

B. Interference of Bethe-Heitler and DVCS amplitudes

Next, let us present approximate results for the interference term which is the most promising observable for the phenomenology of GPDs since it is linear in CFFs. This property simplifies the disentanglement of CFFs from experimental measurements. The Fourier harmonics have the form:

$$c_0^{\mathcal{I}} = -8(2-y)\Re{\rm e}\Big\{\frac{(2-y)^2}{1-y}K^2 + \frac{t}{\mathcal{Q}^2}(1-y)(2-x_{\rm B})\Big\}\mathcal{C}^{\mathcal{I}}(\mathcal{H}), \tag{3.8}$$

$$\begin{Bmatrix} c_1^{\mathcal{I}} \\ s_1^{\mathcal{I}}\end{Bmatrix} = 8K\begin{Bmatrix}-(2-2y+y^2)\Re{\rm e} \\ \lambda y(2-y)\Im{\rm m}\end{Bmatrix}\mathcal{C}^{\mathcal{I}}(\mathcal{H}), \tag{3.9}$$

[2]We adopt here the notation of Ref. [10] rather than of Ref. [14].

[3]These were omitted in our earlier consideration [14] of DVCS on spinless targets since they enter the amplitudes suppressed by a power of the QCD coupling constant. Note that $\mathcal{H}_T$ also enters as an $(\alpha_s/\pi)^2$ suppressed contribution to $c_0^{\rm DVCS}$ and as an α_s/π suppressed effect in the twist-three harmonics $c_1^{\rm DVCS}$ and $s_1^{\rm DVCS}$, cf. Eq. (3.6).

$$\begin{Bmatrix} c_2^I \\ s_2^I \end{Bmatrix} = \frac{16K^2}{2-x_{\rm B}} \begin{Bmatrix} -(2-y)\Re{\rm e} \\ \lambda y \Im{\rm m} \end{Bmatrix} \mathcal{C}^I(\mathcal{H}^{\rm eff}), \tag{3.10}$$

$$c_3^I = -\frac{8\mathcal{Q}^2K^3}{M^2(2-x_{\rm B})^2}\Re{\rm e}\mathcal{C}_T^I(\mathcal{H}_T). \tag{3.11}$$

Explicit calculations demonstrate that the twist-three harmonics, i.e., c_2^I and s_2^I have the same functional dependence as the twist-two coefficients, c_1^I and s_1^I. However, this is not the case for c_3^I and s_3^I which emerge due to gluon helicity-flip CFF $\mathcal{H}_T$,

$$\mathcal{C}^I(\mathcal{H}) = F\mathcal{H}, \qquad \mathcal{C}_T^I = F\mathcal{H}_T. \tag{3.12}$$

This set of formulas forms the complete result for the real-photon leptoproduction cross section in the twist-three approximation.

IV. HELICITY AMPLITUDES

The consideration of the previous section was restricted to the twist-three approximation for the dynamical as well as kinematical effects. Higher-twist operator product expansion analyses of the off-forward Compton scattering amplitude, similar to the one performed for the deeply inelastic scattering [18], is intrinsically involved due to complications and ambiguities in the choice of operator basis. The incorporation of kinematical power-suppressed effects is relatively straightforward. In order to achieve this in the most efficient manner we separate power corrections that arise from the leptonic and hadronic parts by evaluating photon helicity amplitudes utilizing the polarization vectors for the incoming and outgoing photons in the target rest frame as defined in Appendix A in Eqs. (A6) and (A7), respectively.

A. Squared DVCS term

Using the completeness relations (A10) and (A11) for the photon polarization vectors, we can rewrite the square of the DVCS amplitude (2.6) as follows:

$$|\mathcal{T}^{\rm DVCS}|^2 = \frac{1}{\mathcal{Q}^2}\sum_{a=-,0,+}\sum_{b=-,0,+}\mathcal{L}_{ab}(\lambda,\phi)\mathcal{W}_{ab},$$
$$\mathcal{W}_{ab} = \mathcal{T}_{a+}^{\rm DVCS}(\mathcal{T}_{b+}^{\rm DVCS})^* + \mathcal{T}_{a-}^{\rm DVCS}(\mathcal{T}_{b-}^{\rm DVCS})^*, \tag{4.1}$$

in terms of helicity amplitudes labeled by the helicity states of the (initial) photon. These are defined by contractions of the Lorentz-covariant amplitudes with the photon polarization vectors (A6) and (A7),

$$\mathcal{L}_{ab}(\lambda,\phi) = \varepsilon_1^{\mu^*}(a)\mathcal{L}_{\mu\nu}(\lambda)\varepsilon_1^{\nu}(b) \tag{4.2}$$

and

$$\mathcal{T}_{ac}^{\rm DVCS}(\phi) = (-1)^{a-1}\varepsilon_2^{\mu^*}(c)T_{\mu\nu}\varepsilon_1^{\nu}(a), \tag{4.3}$$

where the phase $(-1)^{a-1}$ takes care of the signature factor in the completeness relation (A10).

The helicity amplitudes (4.3) are constrained by the parity conservation and, as a consequence, we have just three independent functions,

$$\mathcal{T}_{++}^{\rm DVCS} = \mathcal{T}_{--}^{\rm DVCS}, \qquad \mathcal{T}_{0+}^{\rm DVCS} = \mathcal{T}_{0-}^{\rm DVCS},$$
$$\mathcal{T}_{-+}^{\rm DVCS} = \mathcal{T}_{+-}^{\rm DVCS}. \tag{4.4}$$

The leptonic helicity amplitudes are calculated exactly from the definitions (2.8) and (A6) and read

$$\mathcal{L}_{++}(\lambda) = \frac{1}{y^2(1+\epsilon^2)}\left(2-2y+y^2+\frac{\epsilon^2}{2}y^2\right) - \frac{2-y}{\sqrt{1+\epsilon^2}y}\lambda, \tag{4.5}$$

$$\mathcal{L}_{00} = \frac{4}{y^2(1+\epsilon^2)}\left(1-y+\frac{\epsilon^2}{4}y^2\right), \tag{4.6}$$

$$\mathcal{L}_{0+}(\lambda,\phi) = \frac{2-y-\lambda y\sqrt{1+\epsilon^2}}{y^2(1+\epsilon^2)} \times\sqrt{2}\sqrt{1-y-\frac{\epsilon^2}{4}y^2}e^{-i\phi}, \tag{4.7}$$

$$\mathcal{L}_{-+}(\phi) = \frac{2}{y^2(1+\epsilon^2)}\left(1-y+\frac{\epsilon^2}{4}y^2\right)e^{-i2\phi}, \tag{4.8}$$

with the remaining ones related to and already found by parity and time-reversal invariance

$$\mathcal{L}_{0-}(\lambda,\phi) = \mathcal{L}_{0+}(-\lambda,-\phi),$$
$$\mathcal{L}_{\pm,0}(\lambda,\phi) = \mathcal{L}_{0,\pm}(-\lambda,\phi),$$
$$\mathcal{L}_{--}(\lambda) = \mathcal{L}_{++}(-\lambda),$$
$$\mathcal{L}_{-+}(\phi) = \mathcal{L}_{+-}(-\phi). \tag{4.9}$$

Using the above relations among helicity amplitudes, we can cast the squared DVCS amplitude in the following form:

$$\begin{aligned}\mathcal{Q}^2|\mathcal{T}^{\rm DVCS}|^2 = {} & 2\mathcal{L}_{++}(\lambda=0)[T_{++}(T_{++})^* + T_{+-}(T_{+-})^*] \\ & + 2\mathcal{L}_{00}T_{0+}(T_{0+})^* + [\mathcal{L}_{0+}(\lambda,\phi) \\ & + \mathcal{L}_{0+}(-\lambda,-\phi)]T_{0+}[T_{++}+T_{+-}]^* \\ & + [\mathcal{L}_{0+}(-\lambda,\phi) + \mathcal{L}_{0+}(\lambda,-\phi)] \\ & \times[T_{++}+T_{+-}](T_{0+})^* + [\mathcal{L}_{+-}(\lambda,\phi) \\ & + \mathcal{L}_{+-}(-\lambda,-\phi)][T_{++}(T_{+-})^* \\ & + T_{+-}(T_{++})^*].\end{aligned} \tag{4.10}$$

These findings immediately allow one to get the Fourier coefficients in the refined approximation. Substituting the hadronic helicity amplitudes computed to the twist-three accuracy from Lorentz-covariant parametrizations of the Compton tensor from Sec. VA,

$$\mathcal{T}^{\rm DVCS}_{++} = \mathcal{H} + \mathcal{O}(1/\mathcal{Q}^2), \tag{4.11}$$

$$\mathcal{T}^{\rm DVCS}_{0+} = \frac{\sqrt{2}}{2-x_{\rm B}}\frac{\tilde{K}}{\mathcal{Q}}\mathcal{H}^{\rm eff}_3 + \mathcal{O}(1/\mathcal{Q}^3) + \mathcal{O}(\alpha_s/\mathcal{Q}), \tag{4.12}$$

$$\mathcal{T}^{\rm DVCS}_{-+} = \frac{2}{(2-x_{\rm B})^2}\frac{\tilde{K}^2}{M^2}\mathcal{H}_T + \mathcal{O}(1/\mathcal{Q}^2), \tag{4.13}$$

where the effective twist-three CFF $\mathcal{H}^{\rm eff}_3$ was defined earlier in Eq. (3.7), we can read off the kinematically improved DVCS harmonics,

$$c_0^{\rm DVCS} = 2\frac{2-2y+y^2+\frac{\epsilon^2}{2}y^2}{1+\epsilon^2}\mathcal{C}^{\rm DVCS}(\mathcal{H},\mathcal{H}^*;\mathcal{H}_T,\mathcal{H}_T^*) + \frac{16K^2\mathcal{H}_{\rm eff}\mathcal{H}^*_{\rm eff}}{(2-x_{\rm B})^2(1+\epsilon^2)}, \tag{4.14}$$

$$\begin{Bmatrix} c_1^{\rm DVCS} \\ s_1^{\rm DVCS}\end{Bmatrix} = \frac{8K}{(2-x_{\rm B})(1+\epsilon^2)} \times \begin{Bmatrix} (2-y)\Re{\rm e} \\ -\lambda y\sqrt{1+\epsilon^2}\Im{\rm m}\end{Bmatrix}\mathcal{C}^{\rm DVCS}(\mathcal{H}^{\rm eff};\mathcal{H}^*;\mathcal{H}_T^*), \tag{4.15}$$

$$c_2^{\rm DVCS} = \frac{16\mathcal{Q}^2K^2}{M^2(2-x_{\rm B})^2(1+\epsilon^2)}\Re{\rm e}\mathcal{C}_T^{\rm DVCS}(\mathcal{H},\mathcal{H}_T^*). \tag{4.16}$$

Here the $\mathcal{C}$ functions are the same as those that appeared in Eqs. (3.6). Thus, to restore the power-suppressed contribution in the leptonic part it suffices to perform the following substitutions, found by comparing Eqs. (3.3), (3.4), and (3.5) with (4.14), (4.15), and (4.16):

$$\begin{aligned} 2-2y+y^2 &\Rightarrow \frac{2-2y+y^2+\frac{\epsilon^2}{2}y^2}{1+\epsilon^2}, \\ \begin{Bmatrix}2-y\\ -\lambda y\end{Bmatrix} &\Rightarrow \frac{1}{1+\epsilon^2}\begin{Bmatrix}2-y\\ -\lambda y\sqrt{1+\epsilon^2}\end{Bmatrix}, \\ \frac{\mathcal{Q}^2K^2}{M^2} &\Rightarrow \frac{\mathcal{Q}^2K^2}{M^2(1+\epsilon^2)}. \end{aligned} \tag{4.17}$$

B. Interference terms

Finally let us turn to improving the interference $\mathcal{I}$ by treating it in the manner completely analogous to the previous consideration for the squared DVCS term. As a result, one finds

$$\mathcal{I} = \frac{\pm e^6}{t\mathcal{P}_1(\phi)\mathcal{P}_2(\phi)}F(t)\sum_{a=-,0,+}\sum_{b=-,+}\{\mathcal{L}^P_{ab}(\lambda,\phi)T_{ab} + (\mathcal{L}^P_{ab}(\lambda,\phi)T_{ab})^*\}, \tag{4.18}$$

where the leptonic part reads

$$\mathcal{L}^P_{ab}(\lambda,\phi) = \epsilon_1^{\mu*}(a)L_{\mu\nu\tau}(p_1+p_2)^\nu\epsilon_2^\tau(b), \tag{4.19}$$

while the definition of the hadronic amplitude is self-obvious. In the present formalism, the angular dependence is entirely contained in the leptonic part and is rather intricate. Rewriting the interference in the form

$$\mathcal{I} = \frac{\pm e^6F(t)}{t\mathcal{P}_1(\phi)\mathcal{P}_2(\phi)}[(\mathcal{L}^P_{++}+\mathcal{L}^P_{--})T_{++} + (\mathcal{L}^P_{0+}+\mathcal{L}^P_{0-})T_{0+} + (\mathcal{L}^P_{-+}+\mathcal{L}^P_{+-})T_{-+} + {\rm c.c.}],$$

we introduce the decomposition of the leptonic amplitudes in Fourier harmonics encoding the azimuthal dependence,

$$\mathcal{L}^P_{+a+b} + \mathcal{L}^P_{-a-b} = -\frac{1}{2x_{\rm B}y^3}\Big\{\sum_{n=0}^{3}C_{ab}(n)\cos(n\phi) + i\lambda\sum_{n=1}^{2}S_{ab}(n)\sin(n\phi)\Big\}. \tag{4.20}$$

The explicit expressions for the exact Fourier coefficients in the leptonic tensor are given in Appendix B. Notice that once one computes the leptonic part exactly rather than to the twist-three accuracy, as was done in Sec. III, the simple one-to-one relation between Fourier coefficients and twist expansion in terms of CFFs is lost beyond the $1/\mathcal{Q}^2$ accuracy. This does not prevent one, however, to project out the real and imaginary parts of separate CFFs.

C. How robust is leading approximation for harmonics?

As we will demonstrate in this section, differences between the approximate and exact amplitudes can be quite significant due to numerical enhancements of power-suppressed contributions in the valence and large-$x_{\rm B}$ kinematical regions. We ignore the helicity-flip amplitudes in our consideration and focus our attention on the consequences of the improvements in the twist-two sector encoded into the approximate Fourier coefficients c_1^I and s_1^I in Eq. (3.9). At first let us propose a "hot fix" which is an approximation to the exact result and accounts for the most significant source of enhanced kinematical corrections, on the one hand, but leaves dynamical corrections out of the picture, on the other. This constitutes in the replacements

$$8K\begin{Bmatrix}-(2-2y+y^2)\\ \lambda y(2-y)\end{Bmatrix} \Rightarrow \begin{Bmatrix}C_{++}(n=1)\\ \lambda S_{++}(n=1)\end{Bmatrix} \tag{4.21}$$

in Eq. (3.9). The admixture of higher harmonics proportional to $\mathcal{H}$ is not large for the present experiments, however, one should take care of the zero harmonics by the substitution in (3.8)

$$-8(2-y)\Big\{\frac{(2-y)^2}{1-y}K^2 + \frac{t}{\mathcal{Q}^2}(1-y)(2-x_{\rm B})\Big\} \Rightarrow C_{++}(n=0). \tag{4.22}$$

Notice that in this approximation the constant contribution,

suppressed by the power of $1/\mathcal{Q}$ compared to the first harmonics, is entirely determined by the twist-two CFFs $\mathcal{H}$.

This hot fix provides a significant improvement of the leading approximation, as demonstrated in Fig. 3 where we compared it with exact formulas using for illustrative purposes the target with the mass $M = 0.94$ GeV. There, in the left and right panels, we present the plots for the typical kinematical setups, with relatively large values of t', of the present JLab ($E_e = 5.7$ GeV),

$$t' = -0.3\ \text{GeV}^2, \qquad x_B = 0.3, \qquad \mathcal{Q}^2 = 1.5\ \text{GeV}^2, \tag{4.23}$$

and HERMES ($E_e = 27.5$ GeV),

$$t' = -0.3\ \text{GeV}^2, \qquad x_B = 0.1, \qquad \mathcal{Q}^2 = 2.5\ \text{GeV}^2 \tag{4.24}$$

experiments, respectively. A naked eye inspection of the plots of the low-$\mathcal{Q}$/high-x_B JLab kinematics exhibits the evident feature that the approximation (3.8) and (3.9) (shown by dotted curves) provides a sizeable false enhancement effect of the leading twist harmonics compared with the exact result (solid lines). Fortunately, the contamination by higher harmonics is small and so the substitutions (4.22)−(4.21) provide already a good agreement with exact results (dashed line in Fig. 3). For low-$\mathcal{Q}^2$/large-x_B, we find ∼30% and ∼70% deviations for the first odd and even harmonics in the angle ϕ, respectively. For HERMES, where x_B is smaller and $\mathcal{Q}^2$ larger, the approximations (3.8) and (3.9) are justified as it is obvious from Fig. 3. We note, however, that also for this kinematics at larger values of x_B one may find relative deviations from the exact results of the order of 15% or so.

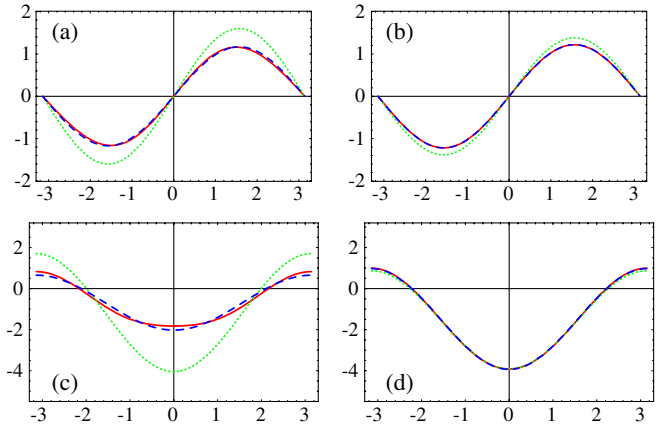

FIG. 3 (color online). Odd (a), (b) and even (c), (d) harmonics of the interference term (3.2) versus ϕ as they arise from the helicity nonflip distribution amplitude $\mathcal{T}_{++}$ (set to one) for JLab (a), (c) and HERMES (c), (d) kinematics as specified in Eqs. (4.23) and (4.24), respectively. The dotted and dashed curves emerge from $s_1 \sin(\phi)$ and $c_0 + c_1 \cos(\phi)$ in the approximations of Eqs. (3.8), (3.9), (4.21), and (4.22), respectively, while the solid ones contain all harmonics (4.26) and (4.27).

One should also be concerned about the size of twist-three effects, originating from the longitudinal-transverse helicity amplitude $T_{0\pm}$. They are formally suppressed by $\sqrt{-t'/Q}$ and show up in higher harmonics in the leading approximation of Sec. III, which, however, are kinematically contaminated by lower ones when computed exactly. For instance, for the JLab kinematics (4.23) we find

$$\begin{aligned}\mathcal{I} \propto & -1.34[\cos(\phi) + 0.51 - 0.14\cos(2\phi)]\Re\mathrm{e}\mathcal{H} \\ & - 0.68[\cos(2\phi) - 0.32 + 0.21\cos(\phi)]\Re\mathrm{e}\mathcal{H}_3^{\text{eff}} \\ & + 1.16\lambda[\sin(\phi) + 0.04\sin(2\phi)]\Im\mathrm{m}\mathcal{H} \\ & + 0.23\lambda[\sin(2\phi) + 0.79\sin(\phi)]\Im\mathrm{m}\mathcal{H}_3^{\text{eff}}. \end{aligned} \tag{4.25}$$

If the twist-tree CFF $\mathcal{H}_3^{\text{eff}}$ is comparable in magnitude to the twist-two $\mathcal{H}$, it may provide a sizeable contribution to the lower harmonics, i.e., $\sin(\phi)$, $\cos(\phi)$, and the constant part. The size of the $\sin(2\phi)$ and $\cos(2\phi)$ harmonics will serve as an accurate estimate of this admixture. Note that for (very) small values of $\sqrt{-t'/Q}$, the twist-two and twist-three harmonics start to decouple. However, even for HERMES kinematics one must account for these mixing effects for average values of $-t \sim 0.3$ GeV^2.

Finally, we mention that in the present estimate (4.25) we ignored the transverse-transverse helicity-flip amplitude T_{+-} since it safely decouples from the other ones. It shows up in the $\cos(3\phi)$ harmonics, which is only slightly affected by the twist-two and twist-three CFFs. On the other hand, its contribution to the lower harmonics is negligible.

Since the ultimate goal of the exclusive cross section (2.1) measurements is the extraction of CFFs and consequently clean separation of GPDs, which shed light on the internal structure of hadrons, data analyses have to disentangle the intricate dependence of kinematical factors on dynamical variables from the one of GPDs themselves. Therefore, the role of $1/\mathcal{Q}$ power-suppressed contributions should not be underestimated as these enter dressed with numerically enhanced factors being a function of y, x_B, and t. Therefore, for the most robust CFF extraction, we suggest to utilize the following general formulas for the Fourier coefficients in data analyses

$$\begin{aligned} c_n^{\mathcal{I}} = & C_{++}(n)\Re\mathrm{e}\mathcal{C}^{\mathcal{I}}(\mathcal{H}) + \frac{\sqrt{2}}{2 - x_B}\frac{\tilde{K}}{\mathcal{Q}} C_{0+}(n)\Re\mathrm{e}\mathcal{C}^{\mathcal{I}}(\mathcal{H}_3^{\text{eff}}) \\ & + \frac{2}{(2 - x_B)^2}\frac{\tilde{K}^2}{M^2} C_{-+}(n)\Re\mathrm{e}\mathcal{C}^{\mathcal{I}}(\mathcal{H}_T), \end{aligned} \tag{4.26}$$

$$s_n^I = S_{++}(n)\Im\mathrm{m}\mathcal{C}^I(\mathcal{H}) + \frac{\sqrt{2}}{2-x_B} \times \frac{\tilde{K}}{\mathcal{Q}} S_{0+}(n)\Im\mathrm{m}\mathcal{C}^I(\mathcal{H}_3^{\mathrm{eff}}) + \frac{2}{(2-x_B)^2} \times \frac{\tilde{K}^2}{M^2} S_{-+}(n)\Im\mathrm{m}\mathcal{C}^I(\mathcal{H}_T), \quad (4.27)$$

in the interference term (3.2). Though this results into a more involved extraction procedure, compared to that one described in Ref. [10], it will not introduce any complications of principle.

V. UNCERTAINTIES ARISING FROM THE TWIST EXPANSION

There are various possibilities to write down the tensor decomposition for the DVCS tensor (1.1) respecting its gauge invariance and Lorentz covariance. Each of them will be associated with a specific set of CFFs. Of course, all parametrizations are equivalent. However, relating physical CFFs to partonic GPDs requires an expansion in inverse powers of the hard scale $\mathcal{Q}$, known as the twist expansion. As a consequence, expressions obtained for different parametrizations will only be equivalent to the considered order in the $1/\mathcal{Q}$ expansion and differ when higher order terms are taken into account. Let us address several Lorentz structures used in the literature and discuss their manifestation in physical observables.

Presently, the hadronic Compton amplitude (1.1) has been worked out to the twist-three accuracy within the GPD formalism [5–9]. While the leading twist sector is known in the next-to-leading [19] and next-to-next-to-leading [20] orders in the modified minimal subtraction and the special conformal subtraction schemes, respectively, the twist-three coefficient functions are available in the handbag approximation only (with a partial one-loop calculation reported in Ref. [21]). The restriction of the current analyses to account for $1/\mathcal{Q}$ suppressed effects is a drawback which yields insufficient accuracy to render the DVCS tensor gauge invariant and obey the transversality condition, arising from the current conservation,

$$q_1^\nu T_{\mu\nu} = q_2^\mu T_{\mu\nu} \equiv 0, \quad (5.1)$$

exactly. To illustrate the interplay of higher-twist contributions and the restoration of the transversality condition of the DVCS tensor, let us recall the role of the twist-three effects in this endeavor. For a scalar target, the twist-two result in the handbag approximation reads:

$$T^{(2)}_{\mu\nu} = -\frac{1}{p\cdot q}[(p\cdot q)g_{\mu\nu} - q_\mu p_\nu - q_\nu p_\mu - \xi p_\mu p_\nu]\mathcal{H}(\xi,t;\mathcal{Q}^2), \quad (5.2)$$

where we used the symmetric variables $p = p_1 + p_2$ and $q = \frac{1}{2}(q_1 + q_2)$ which spawn the generalized Bjorken variable $\xi = Q^2/p\cdot q$ defined in terms of the average photon virtuality $Q^2 = -q^2$. In the nonforward kinematics of DVCS, obviously this tensor does not respect the current conservation and so one finds after contraction, e.g., with q_2^μ, that the transversality condition (5.1) is violated by $\Delta_\nu^\perp = \Delta_\nu - \eta p_\nu$ which, according to the power counting, is a twist-three effect. The variable η is the t-channel scaling variable known as skewness $\eta = (\Delta\cdot q)/(p\cdot q)$. It is related to the generalized Bjorken variable ξ for the DVCS kinematics via the relation $\eta = -\xi/(1 + t/2\mathcal{Q}^2) \approx -\xi$. Evaluation of the twist-three amplitudes yields beside a contribution proportional to the function $\mathcal{H}_3$

$$T^{(3)}_{\mu\nu} = \frac{1}{p\cdot q}[\Delta_\mu^\perp(q_{2\nu} + \xi p_\nu) + \Delta_\nu^\perp(q_{1\mu} + \xi p_\mu)]\mathcal{H}_3, \quad (5.3)$$

also an antisymmetric tensor accompanied by the twist-two CFF $\mathcal{H}$

$$\delta T^{(2)} = \frac{1}{p\cdot q}[\Delta_\mu^\perp p_\nu - \Delta_\nu^\perp p_\mu]\mathcal{H}.$$

The latter when combined with Eq. (5.2), $T^{(2)} + \delta T^{(2)}$, generates the replacement of the twist-two Lorentz structure with

$$-(p\cdot q)g_{\mu\nu} + q_\mu p_\nu + q_\nu p_\mu + \xi p_\mu p_\nu \to -(p\cdot q)g_{\mu\nu} + q_{1\mu} p_\nu + q_{2\nu} p_\mu + \xi p_\mu p_\nu.$$

It is straightforward to check now that the violation of the transversality condition is postponed to the twist-four level, i.e., $\mathcal{O}(\mathcal{Q}^{-2})$. Thus addressing it requires a full-fledged twist-four analysis along the lines of Ref. [18]. Since such a calculation has not been performed yet in a consistent manner, we will take a pragmatic point of view and restore the exact gauge invariance in several superficially inequivalent ways and study the resulting numerical differences.

A. Lorentz decomposition of the Compton tensor

The complete twist-three result for the DVCS tensor for a scalar target has three independent CFFs, which is the maximal possible number allowed by the underlying symmetries. The result reads in terms of physical four-momenta as follows:

$$T^{(2+3)}_{\mu\nu} = -\frac{1}{(p\cdot q)}[(p\cdot q)g_{\mu\nu} - q_{1\mu}p_\nu - q_{2\nu}p_\mu - \xi p_\mu p_\nu]\left(\mathcal{H} + \frac{\Delta_\perp^2}{2M^2}\mathcal{H}_{\rm T}\right) + \frac{1}{M^2}\Delta_{\perp\mu}\Delta_{\perp\nu}\mathcal{H}_{\rm T} + \frac{1}{(p\cdot q)}[\Delta_{\perp\mu}(q_{2\nu} + \xi p_\nu) + \Delta_{\perp\nu}(q_{1\mu} + \xi p_\mu)]\mathcal{H}_3. \tag{5.4}$$

As mentioned above the two Lorentz tensors, proportional to the CFFs $\mathcal{H}$ and $\mathcal{H}_3$, are transverse up to twist-four terms. The third structure is a symmetric and traceless tensor, which is induced by the gluon transversity (photon helicity flip by two units) [22–24]. It is only transversal to the order $\Delta_\perp/M$.

Utilizing the equation of motion at twist-four level should allow one to satisfy the transversality condition (5.1) exactly, since the higher than geometric twist-four contributions are formally absent in the handbag diagram being proportional to derivatives of Dirac delta function. The restoration of the transversality condition for the Lorentz structures, proportional to $\mathcal{H}$ and $\mathcal{H}_3$ requires a t-dependent term, since neglecting such terms results in a failure of (5.1) [25]. The "minimalist" restoration in the twist-two sector requires to add a $(t/Q^2)p_\mu p_\nu$ contribution, leading to the replacement

$$(p\cdot q)g_{\mu\nu} - q_{1\mu}p_\nu - q_{2\nu}p_\mu - \xi p_\mu p_\nu \to (p\cdot q)g_{\mu\nu} - q_{1\mu}p_\nu - q_{2\nu}p_\mu - \left(1 + \frac{t}{4Q^2}\right)\xi p_\mu p_\nu. \tag{5.5}$$

In the twist-three sector one needs a

$$\frac{t}{Q^2}\frac{q_\mu p_\nu - q_\nu p_\mu + \eta p_\mu p_\nu}{p\cdot q}$$

proportional term, which can be absorbed by adding power-suppressed contributions to the following four-vectors:

$$\Delta_{\perp\mu} \to \Delta_{\perp\mu} \pm \frac{t}{2Q^2}\xi p_\mu, \qquad q_{i\mu} + \xi p_\mu \to q_{i\mu} + \left(1 + \frac{t}{4Q^2}\right)\xi p_\mu, \tag{5.6}$$

with $\pm$ sign in the first equation standing for indices associated with outgoing/incoming photons. The restoration of the gauge invariance for the gluon transversity is more cumbersome, since it will already be affected at the twist-three level. It can be achieved by adding a $\Delta_\perp$ proportional term [17]. For later illustration we adopt here the recipes (5.5) and (5.6). Finally, the DVCS tensor can then be written as

$$T_{\mu\nu} = -\frac{1}{p\cdot q}\Big[(p\cdot q)g_{\mu\nu} - q_{1\mu}p_\nu - q_{2\nu}p_\mu - \left(1 + \frac{t}{4Q^2}\right)\xi p_\mu p_\nu\Big]\left(\mathcal{H} + \frac{\Delta_\perp^2}{2M^2}\mathcal{H}_{\rm T}\right) + \frac{1}{M^2}\left(\Delta_{\perp\mu} + \frac{t}{2Q^2}\xi p_\mu\right)\left(\Delta_{\perp\nu} - \frac{t}{2Q^2}\xi p_\nu\right)\mathcal{H}_{\rm T} + \frac{1}{p\cdot q}\Big[\left(q_{2\nu} + \left(1 + \frac{t}{4Q^2}\right)\xi p_\nu\right)\left(\Delta_{\perp\mu} + \frac{t}{2Q^2}\xi p_\mu\right) + \left(q_{1\mu} + \left(1 + \frac{t}{4Q^2}\right)\xi p_\mu\right)\left(\Delta_{\perp\nu} - \frac{t}{2Q^2}\xi p_\nu\right)\Big]\mathcal{H}_3. \tag{5.7}$$

For DVCS kinematics this parametrization is complete and, thus, it can be uniquely mapped into a different form, e.g., used in Ref. [26].

Another way to restore gauge invariance of the amplitude (1.1) beyond twist-three accuracy is by introducing a projector [7]

$$\mathcal{P}^{\mu\nu} \equiv g^{\mu\nu} - \frac{q_1^\mu q_2^\nu}{q_1\cdot q_2}, \tag{5.8}$$

fulfilling the conditions $\mathcal{P}^{\mu\nu}q_{1\nu} = q_{2\mu}\mathcal{P}^{\mu\nu} = 0$. They provide a transverse Compton tensor when contracted on both sides with the twist-two DVCS amplitude $T^{(2)}_{\mu\nu}$. When expanded to twist-three accuracy this procedure reproduces gauge-restoring terms coinciding with the ones obtained from the explicit analysis reviewed in the preamble to Sec. V. Notice, however, that contrary to the consideration in the previous paragraph, this recipe generates an infinite tower of higher-twist contributions when expanded in inverse powers of the average photon virtuality.

Finally, let us address the formalism of Ref. [27]. In applications of the QCD-improved parton model to high-energy scattering, it is customary to parametrize the Compton tensor in terms of the light-cone vector n^μ and its tangent $\tilde{n}^\mu$ such that $n^2 = \tilde{n}^2 = 0$ and $n\cdot\tilde{n} = 1$. In particular, these can be chosen as the plus and minus components of the initial photon and proton momenta, respectively, cf. Figure 2. However, the choice of the light-cone vectors is not unique, since it implicitly refers to a given reference frame. For instance, the parametrization used in Ref. [27],

$$q_{1\mu} = \frac{Q^2}{4\xi'}n_\mu - 2\xi'\tilde{n}_\mu, \qquad p_\mu = 2\tilde{n}_\mu + \frac{4M^2 - t}{2}n_\mu, \qquad \Delta_\mu = -(2\bar{\xi})\tilde{n}_\mu + \bar{\xi}\frac{4M^2 - t}{4}n_\mu + \bar{\Delta}_{\perp\mu}, \tag{5.9}$$

is done in a "collinear" frame ($\vec{p}_{1\perp} = -\vec{p}_{2\perp}$). We note that the scaling variables ξ' and $\bar{\xi}$ are proportional to the generalized Bjorken variable ξ and skewness $\eta \simeq -\xi$, respectively, but, differ from them by power-suppressed

corrections. The DVCS tensor parametrized in terms of the light-cone vectors rather than physical four-vectors reads [27]

$$T_{\mu\nu} = -\left[g_{\mu\nu} - n_\mu\tilde{n}_\nu - \tilde{n}_\mu n_\nu + \frac{\tilde{n}_\mu \bar{\Delta}_{\perp\nu}}{\tilde{n}\cdot q_2}\right]\mathcal{H} + \left[\bar{\Delta}_{\perp\mu} + \bar{\Delta}^2_\perp \frac{\tilde{n}_\mu}{\tilde{n}\cdot q_2}\right]\left[\frac{n_\nu}{2} + 4\xi'^2\frac{\tilde{n}_\nu}{\mathcal{Q}^2}\right]\mathcal{H}_3 + \left[\frac{\bar{\Delta}_{\perp\mu}\bar{\Delta}_{\perp\nu}}{M^2} - \frac{\bar{\Delta}^2_\perp}{2M^2}\left(g_{\mu\nu} - n_\mu\tilde{n}_\nu - \tilde{n}_\mu n_\nu - \frac{\tilde{n}_\mu\bar{\Delta}_{\perp\nu}}{\tilde{n}\cdot q_2}\right)\right]\mathcal{H}_{\mathrm{T}}. \tag{5.10}$$

In the first and third Lorentz structure the linear term $\bar{\Delta}_{\perp\nu}$ exactly restores the transversality, while for the second Lorentz structure a $\bar{\Delta}^2$-proportional term is needed. Note that the restoration of transversality for the gluon transversity-induced Lorentz structure essentially differs from the prescription employed in the parametrization (5.7). In the frame we are adopting, the transversal helicity amplitudes, $\gamma^*_T \to \gamma_T$, are given by CFFs $\mathcal{H}$ and $\mathcal{H}_T$, while the longitudinal one, $\gamma^*_L \to \gamma_T$, is entirely related to the twist-three CFF $\mathcal{H}_3$.

To get rid of the frame dependence in the parametrization (5.10), we use the relations (5.9) to express the DVCS tensor in terms of the physical momenta. After this, the tensor takes a frame-independent Lorentz-covariant form. Comparing it to the parametrization (5.7) we can read off a rather cumbersome relation among the two sets of CFFs.

B. Numerical estimates

The leading contribution to each hadronic helicity amplitude from any tensor decomposition, either (5.4), (5.7), or (5.10), is universal and is given by Eqs. (4.11), (4.12), and (4.13). Differences will arise starting with $1/\mathcal{Q}^2$ contributions. To illustrate uncertainties related to the twist-four effects we evaluate the helicity amplitudes to the order $1/\mathcal{Q}^3$. The differences in the helicity conserved amplitude from the calculated (5.4) and improved (5.7) DVCS tensor is

$$\mathcal{T}^{\mathrm{DVCS}}_{++}|_{\mathrm{Eq.\ (5.4)}} - \mathcal{T}^{\mathrm{DVCS}}_{++}|_{\mathrm{Eq.\ (5.7)}} \simeq \mathcal{O}\left(\frac{x_{\mathrm{B}}^2 t t'}{\mathcal{Q}^4}\right). \tag{5.11}$$

It can be considered as negligible and plays practically no role. The ambiguities in the restoration of transversality with (5.4) shows up mainly in the gluon transversity-induced sector yielding

$$\mathcal{T}^{\mathrm{DVCS}}_{++}|_{\mathrm{Eq.\ (5.10)}} - \mathcal{T}^{\mathrm{DVCS}}_{++}|_{\mathrm{Eq.\ (5.7)}} = \frac{(4M^2 - t)x_{\mathrm{B}}^3 4(1 - x_{\mathrm{B}})x_{\mathrm{B}}M^2 - (4 - 3x_{\mathrm{B}})t}{(2 - x_{\mathrm{B}})^4 M^2}\mathcal{H}_{\mathrm{T}} + \mathcal{O}(1/\mathcal{Q}^4). \tag{5.12}$$

It is suppressed for small x_{B} by a factor x_{B}^3. The CFFs $\mathcal{H}$ and $\mathcal{H}_3$ enter here as a $x_{\mathrm{B}}^2 t t'/\mathcal{Q}^4$ and $x_{\mathrm{B}}^4 M^2 t'/\mathcal{Q}^4$ suppressed contributions, which are practically very small.

For the longitudinal-transverse helicity amplitude, the higher-twist effects are more pronounced and yield the difference

$$\mathcal{T}^{\mathrm{DVCS}}_{0+}|_{\mathrm{Eq.\ (5.4)}} - \mathcal{T}^{\mathrm{DVCS}}_{0+}|_{\mathrm{Eq.\ (5.7)}} = \frac{x_{\mathrm{B}}\tilde{K}t}{2\sqrt{2}(2 - x_{\mathrm{B}})\mathcal{Q}^3}\left(\mathcal{H}[1 + \mathcal{O}(1/\mathcal{Q}^2)] - 2\frac{1 - 2x_{\mathrm{B}}}{2 - x_{\mathrm{B}}}\mathcal{H}_3[1 + \mathcal{O}(1/\mathcal{Q}^2)]\right) + \frac{\tilde{K}}{\mathcal{Q}}\frac{2M^2x_{\mathrm{B}}^2 - t(2 - 2x_{\mathrm{B}} + x_{\mathrm{B}}^2)}{\sqrt{2}M^2(2 - x_{\mathrm{B}})^3}\mathcal{H}_{\mathrm{T}}[1 + \mathcal{O}(1/\mathcal{Q}^2)]. \tag{5.13}$$

While the two recipes (5.7) and (5.10) yield $x_{\mathrm{B}}(4M^2 - t)\mathcal{H}^{\mathrm{eff}}_3/4\mathcal{Q}^2$, $x_{\mathrm{B}}^2(4M^2 - t)\mathcal{H}^{\mathrm{eff}}/4\mathcal{Q}^2$, and $x_{\mathrm{B}}^2(4M^2 - t)\mathcal{H}_{\mathrm{T}}/4\mathcal{Q}$ suppressed differences.

Finally, for the transverse-transverse helicity-flip amplitude, we find that the ambiguities due to kinematical higher-twist corrections enter at order $1/\mathcal{Q}^4$ for the recipe (5.7), i.e.,

$$\mathcal{T}^{\mathrm{DVCS}}_{-+}|_{\mathrm{Eq.\ (5.4)}} - \mathcal{T}^{\mathrm{DVCS}}_{-+}|_{\mathrm{Eq.\ (5.7)}} \sim O(1/\mathcal{Q}^4), \tag{5.14}$$

however, only at order $1/\mathcal{Q}^2$ for the prescription (5.10).

To give a numerical example demonstrating the contamination of the leading contribution by the ambiguities of the power-suppressed effects, let us start with the JLab kinematics (4.23). Numerically, we find that the nonflip helicity amplitude can be safely approximated by the CFF $\mathcal{H}$, cf. Equation (4.11):

$$\mathcal{T}^{\mathrm{DVCS}}_{++} = \begin{Bmatrix}0.997\\0.996\\1.003\end{Bmatrix}\mathcal{H} + \begin{Bmatrix}0.010\\0.011\\0.008\end{Bmatrix}\mathcal{H}_3 + \begin{Bmatrix}0.019\\0.019\\0.000\end{Bmatrix}\mathcal{H}_T \quad \text{for} \begin{Bmatrix}\text{Eq. (5.4)}\\\text{Eq. (5.7)}\\\text{Eq. (5.10)}\end{Bmatrix}. \tag{5.15}$$

Certainly, here we can practically set $\mathcal{T}^{\mathrm{DVCS}}_{++} = \mathcal{H}$. Unfortunately, for the longitudinal-transverse helicity-flip amplitude we find rather strong deviations from the leading approximation (4.12) that are caused by kinematical corrections:

$$\frac{(2-x_B)\mathcal{Q}\mathcal{T}_{0+}^{\mathrm{DVCS}}}{\sqrt{2}\tilde{K}} = \begin{Bmatrix} 1.30 \\ 1.34 \\ 0.91 \end{Bmatrix} \mathcal{H}_3^{\mathrm{eff}} + \begin{Bmatrix} -0.21 \\ -0.17 \\ 0.02 \end{Bmatrix} \mathcal{H} - \begin{Bmatrix} 0.16 \\ 0.34 \\ 0.03 \end{Bmatrix} \mathcal{H}_T \quad \text{for} \begin{Bmatrix} \text{Eq. (5.4)} \\ \text{Eq. (5.7)} \\ \text{Eq. (5.10)} \end{Bmatrix}. \tag{5.16}$$

Although the effect of restoration of the transversality from the twist-two amplitude (5.4) is small within the recipe (5.7) (except for the gluon transversity), the numerical values deviate considerably for (5.10). We suggest to rely for simplicity on the leading approximation (4.12). Finally, for the transverse-transverse helicity-flip amplitude we again observe that the deviations from the leading approximation (4.13) are negligible except for the parametrization (5.10):

$$\frac{(2-x_B)^2 M\mathcal{T}_{-+}^{\mathrm{DVCS}}}{2\tilde{K}^2} = \begin{Bmatrix} 1.01 \\ 1.00 \\ 0.81 \end{Bmatrix} \mathcal{H}_T + \begin{Bmatrix} -0.02 \\ -0.02 \\ 0.02 \end{Bmatrix} \mathcal{H} - \begin{Bmatrix} 0.06 \\ 0.07 \\ 0.04 \end{Bmatrix} \mathcal{H}_3 \quad \text{for} \begin{Bmatrix} \text{Eq. (5.4)} \\ \text{Eq. (5.7)} \\ \text{Eq. (5.10)} \end{Bmatrix}. \tag{5.17}$$

It is rather obvious that for decreasing x_B and/or increasing $\mathcal{Q}^2$ the "kinematical" power corrections are getting reduced. For instance, for HERMES kinematics (4.24) we find for the most problematic longitudinal-transverse helicity-flip amplitude

$$\frac{(2-x_B)\mathcal{Q}\mathcal{T}_{0+}^{\mathrm{DVCS}}}{\sqrt{2}\tilde{K}} = \begin{Bmatrix} 1.00 \\ 1.03 \\ 1.01 \end{Bmatrix} \mathcal{H}_3^{\mathrm{eff}} + \begin{Bmatrix} -0.02 \\ -0.01 \\ 0.00 \end{Bmatrix} \mathcal{H} + \begin{Bmatrix} 0.05 \\ -0.04 \\ -0.02 \end{Bmatrix} \mathcal{H}_T \quad \text{for} \begin{Bmatrix} \text{Eq. (5.4)} \\ \text{Eq. (5.7)} \\ \text{Eq. (5.10)} \end{Bmatrix}. \tag{5.18}$$

This exhibits the legitimacy of the leading approximation (4.12) employed in Refs. [10,14].

VI. CONCLUSIONS

The main goal of the present consideration was the understanding of the power-suppressed effects in DVCS observables stemming from the exact account for kinematical contributions in the hadronic mass M^2 and momentum transfer t. Using the photon helicity amplitudes, we separated the leptoproduction cross section in terms of the leptonic and hadronic helicity amplitudes. The choice of the target rest frame with the z-axis directed (counter) along to the virtual photon three-momentum allowed one to localize its dependence on the azimuthal angle to the leptonic part. These were then computed exactly to leading order in the QED fine structure constant thus improving approximate results of previous considerations [10,14].

Numerical estimates performed for the current kinematics of JLab experiments demonstrated that, due to rather low virtuality of the hard photon and valence-region values for the Bjorken variable, the restriction to merely the leading approximation of Refs. [10,14] yields a significant overestimate of event rates compared to the exact treatment. However, for higher values of the hard scale, typical for the HERMES experiment, the approximation of the earlier work becomes legitimate. We proposed a set of formulas for the refined analysis of DVCS observables. Although, in the improved approximation the classification scheme of Ref. [10], according to which the Fourier harmonics are strictly associated with the twist of the contributing CFFs, is altered, this does not represent a difficulty of principle to extract CFFs from experimental observables. However, obviously the inversion problem becomes more tedious.

Let us point out that the choice of Lorentz-invariant kinematical variables in the evaluation of CFFs from the corresponding GPDs is also not unique as it has a cross talk with higher-twist contributions. The optimal choice should minimalize $1/\mathcal{Q}^2$-suppressed contributions. This problem was not the focus of our present analysis, where we used as in our previous studies a legitimate choice $\xi = -\eta = x_B/(2-x_B)$ and took the photon virtuality $\mathcal{Q}^2$ as the large scale.

The consideration of the present work can be generalized in a straightforward fashion to targets possessing nonvanishing spin, with nucleon being the most interesting one. We anticipate that our current analysis will quantitatively hold for DVCS off an unpolarized proton target too. The hot fixes (4.17), (4.21), and (4.22), can be immediately used to improve on Eqs. (43)–(45), (54), and (53), respectively, of Ref. [10]. Note that for the spin-one-half target new combinations of CFFs will emerge, e.g., ΔC in the interference term. However, we expect that such contributions, induced by the helicity flip of the outgoing proton, are relatively unimportant for the kinematics of present experiments. We will report on this analysis in future work.

ACKNOWLEDGMENTS

We are indebted to H. Avakian, M. Garçon, M. Guidal, and F. Sabatié for discussions which initiated our studies and to M. Diehl for comments. This work was supported by the U.S. National Science Foundation under Grants No. PHY-0456520 and No. PHY-0757394 and funds provided by the ASU College of Liberal Arts and Sciences. D. M. would like to thank the Particle Physics and Astrophysics Group at ASU for hospitality extended to him during the final stage of the work.

APPENDIX A: KINEMATICS IN THE TARGET REST FRAME

We fix our kinematics by going to the target rest frame and choosing the z component of the virtual photon momentum negative and the x component of the incoming lepton being positive. The components of the corresponding four-vectors read

$$p_1 = (M, 0, 0, 0), \qquad q_1 = \frac{\mathcal{Q}}{\epsilon}(1, 0, 0, -\sqrt{1+\epsilon^2}),$$
$$k = \frac{\mathcal{Q}}{y\epsilon}(1, \sin\theta_l, 0, \cos\theta_l), \tag{A1}$$

with the lepton scattering angle being

$$\cos\theta_l = -\frac{1+\frac{y\epsilon^2}{2}}{\sqrt{1+\epsilon^2}}, \qquad \sin\theta_l = \frac{\epsilon\sqrt{1-y-\frac{y^2\epsilon^2}{4}}}{\sqrt{1+\epsilon^2}}. \tag{A2}$$

The outgoing momenta are parametrized in terms of the scattering angles in the hadronic plane, see Fig. 2,

$$q_2 = \frac{\mathcal{Q}^2 + x_{\rm B} t}{2M x_{\rm B}}(1, \cos\varphi_\gamma \sin\theta_\gamma, \sin\varphi_\gamma \sin\theta_\gamma, \cos\theta_\gamma), \tag{A3}$$

$$p_2 = \Big(M - \frac{t}{2M}, \sqrt{-t+\frac{t^2}{4M^2}}\cos\phi\sin\theta, \sqrt{-t+\frac{t^2}{4M^2}}\sin\phi\sin\theta, \sqrt{-t+\frac{t^2}{4M^2}}\cos\theta\Big), \tag{A4}$$

where the polar angles read in terms of the kinematical variables of the phase space

$$\cos\theta_\gamma = -\frac{1+\frac{\epsilon^2}{2}\frac{\mathcal{Q}^2+t}{\mathcal{Q}^2+x_{\rm B}t}}{\sqrt{1+\epsilon^2}},$$
$$\cos\theta = -\frac{\epsilon^2(\mathcal{Q}^2 - t) - 2x_{\rm B}t}{4x_{\rm B}M\sqrt{1+\epsilon^2}\sqrt{-t+\frac{t^2}{4M^2}}}. \tag{A5}$$

The azimuthal angle of the photon φ_γ is related to the one of the outoing hadron ϕ via $\varphi_\gamma = \phi + \pi$.

The explicit component form of the photon four-momenta allows one to construct their polarization vectors:

$$\varepsilon_1^\mu(\pm) = \frac{e^{\mp i\phi}}{\sqrt{2}}(0, 1, \pm i, 0),$$
$$\varepsilon_1^\mu(0) = \frac{\mathcal{Q}}{\sqrt{2x_{\rm B}}M}(-\sqrt{1+\epsilon^2}, 0, 0, 1), \tag{A6}$$

$$\varepsilon_2^{\mu*}(\pm) = \frac{1}{\sqrt{2}}\Big(0, \frac{1+\frac{\epsilon^2}{2}\frac{\mathcal{Q}^2+t}{\mathcal{Q}^2+x_{\rm B}t}}{\sqrt{1+\epsilon^2}}\cos\phi \pm i\sin\phi, \mp i\cos\phi + \frac{1+\frac{\epsilon^2}{2}\frac{\mathcal{Q}^2+t}{\mathcal{Q}^2+x_{\rm B}t}}{\sqrt{1+\epsilon^2}}\sin\phi, \frac{-\epsilon\mathcal{Q}\tilde{K}/\sqrt{1+\epsilon^2}}{\mathcal{Q}^2+x_{\rm B}t}\Big), \tag{A7}$$

which are defined up to an overall phase factor. The kinematical factor entering the last component of q_2 reads

$$\tilde{K} = \sqrt{t_{\rm min} - t} \times \sqrt{(1-x_{\rm B})\sqrt{1+\epsilon^2} + \frac{(t_{\rm min}-t)(\epsilon^2 + 4(1-x_{\rm B})x_{\rm B})}{4\mathcal{Q}^2}}, \tag{A8}$$

and is related in an obvious manner to K of Eq. (2.12) via

$$K = \sqrt{1 - y + \frac{\epsilon^2}{4}y^2}\,\frac{\tilde{K}}{\mathcal{Q}}. \tag{A9}$$

The photon polarization vectors obey the following completeness relations:

$$\sum_{h=-,+}\varepsilon_1^\mu(h)\varepsilon_1^{\nu*}(h) - \varepsilon_1^\mu(0)\varepsilon_1^\nu(0) = -g^{\mu\nu} + \frac{q_1^\mu q_1^\nu}{q_1^2}, \tag{A10}$$

$$\sum_{h=-,+}\varepsilon_2^\mu(h)\varepsilon_2^{\nu*}(h) = -g^{\mu\nu} + \frac{q_2^\mu p_1^\nu + p_1^\mu q_2^\nu}{p_1\cdot q_2} - \frac{\epsilon^2\mathcal{Q}^2 q_2^\mu q_2^\nu}{(\mathcal{Q}^2 + x_{\rm B}t)^2}, \tag{A11}$$

which are used in the main text to reduce the cross section to the product of helicity amplitudes.

APPENDIX B: FOURIER HARMONICS IN LEPTONIC TENSOR

Let us present explicit expressions for the Fourier coefficients entering the leptonic part of the interference term (4.18). For the transverse-transverse harmonics we found

$$
\begin{aligned}
C_{++}(n=0) &= -\frac{4(2-y)(1+\sqrt{1+\epsilon^2})}{(1+\epsilon^2)^2}\Big\{\frac{\tilde{K}^2}{\mathcal{Q}^2}\frac{(2-y)^2}{\sqrt{1+\epsilon^2}}+\frac{t}{\mathcal{Q}^2}\Big(1-y-\frac{\epsilon^2}{4}y^2\Big)(2-x_{\rm B})\\
&\quad\times\Big(1+\frac{2x_{\rm B}(2-x_{\rm B}+\frac{\sqrt{1+\epsilon^2}-1}{2}+\frac{\epsilon^2}{2x_{\rm B}})\frac{t}{\mathcal{Q}^2}+\epsilon^2}{(2-x_{\rm B})(1+\sqrt{1+\epsilon^2})}\Big)\Big\},\\
C_{++}(n=1) &= \frac{-16K(1-y-\frac{\epsilon^2}{4}y^2)}{(1+\epsilon^2)^{5/2}}\Big\{\Big(1+(1-x_{\rm B})\frac{\sqrt{\epsilon^2+1}-1}{2x_{\rm B}}+\frac{\epsilon^2}{4x_{\rm B}}\Big)\frac{x_{\rm B}t}{\mathcal{Q}^2}-\frac{3\epsilon^2}{4}\Big\}-4K\Big(2-2y+y^2+\frac{\epsilon^2}{2}y^2\Big)\\
&\quad\times\frac{1+\sqrt{1+\epsilon^2}-\epsilon^2}{(1+\epsilon^2)^{5/2}}\Big\{1-(1-3x_{\rm B})\frac{t}{\mathcal{Q}^2}+\frac{1-\sqrt{1+\epsilon^2}+3\epsilon^2}{1+\sqrt{1+\epsilon^2}-\epsilon^2}\frac{x_{\rm B}t}{\mathcal{Q}^2}\Big\},\\
C_{++}(n=2) &= \frac{8(2-y)(1-y-\frac{\epsilon^2}{4}y^2)}{(1+\epsilon^2)^2}\Big\{\frac{2\epsilon^2}{1+\epsilon^2+\sqrt{1+\epsilon^2}}\frac{\tilde{K}^2}{\mathcal{Q}^2}+\frac{x_{\rm B}tt'}{\mathcal{Q}^4}\Big(1-x_{\rm B}-\frac{\sqrt{1+\epsilon^2}-1}{2}+\frac{\epsilon^2}{2x_{\rm B}}\Big)\Big\},\\
C_{++}(n=3) &= -8K\Big(1-y-\frac{\epsilon^2}{4}y^2\Big)\frac{\sqrt{1+\epsilon^2}-1}{(1+\epsilon^2)^{5/2}}\Big\{(1-x_{\rm B})\frac{t}{\mathcal{Q}^2}+\frac{\sqrt{1+\epsilon^2}-1}{2}\Big(1+\frac{t}{\mathcal{Q}^2}\Big)\Big\},\\
S_{++}(n=1) &= -\frac{8K(2-y)y}{1+\epsilon^2}\Big\{1+\frac{1-x_{\rm B}+\frac{\sqrt{1+\epsilon^2}-1}{2}}{1+\epsilon^2}\frac{t'}{\mathcal{Q}^2}\Big\},\\
S_{++}(n=2) &= \frac{4(1-y-\frac{\epsilon^2}{4}y^2)y}{(1+\epsilon^2)^{3/2}}(1+\sqrt{1+\epsilon^2}-2x_{\rm B})\frac{t'}{\mathcal{Q}^2}\Big\{\frac{\epsilon^2-x_{\rm B}(\sqrt{1+\epsilon^2}-1)}{1+\sqrt{\epsilon^2+1}-2x_{\rm B}}-\frac{2x_{\rm B}+\epsilon^2}{2\sqrt{1+\epsilon^2}}\frac{t'}{\mathcal{Q}^2}\Big\},
\end{aligned}
\tag{B1}
$$

while we got for the longitudinal-transverse ones,

$$
\begin{aligned}
C_{0+}(n=0) &= \frac{12\sqrt{2}K(2-y)\sqrt{1-y-\frac{\epsilon^2}{4}y^2}}{(1+\epsilon^2)^{5/2}}\Big\{\epsilon^2+\frac{2-6x_{\rm B}-\epsilon^2}{3}\frac{t}{\mathcal{Q}^2}\Big\},\\
C_{0+}(n=1) &= \frac{8\sqrt{2}\sqrt{1-y-\frac{\epsilon^2}{4}y^2}}{(1+\epsilon^2)^2}\Big\{(2-y)^2\frac{t'}{\mathcal{Q}^2}\Big(1-x_{\rm B}+\frac{(1-x_{\rm B})x_{\rm B}+\frac{\epsilon^2}{4}}{\sqrt{1+\epsilon^2}}\frac{t'}{\mathcal{Q}^2}\Big)\\
&\quad+\frac{1-y-\frac{\epsilon^2}{4}y^2}{\sqrt{1+\epsilon^2}}\Big(1-(1-2x_{\rm B})\frac{t}{\mathcal{Q}^2}\Big)\Big(\epsilon^2-2\Big(1+\frac{\epsilon^2}{2x_{\rm B}}\Big)\frac{x_{\rm B}t}{\mathcal{Q}^2}\Big)\Big\},\\
C_{0+}(n=2) &= -\frac{8\sqrt{2}K(2-y)\sqrt{1-y-\frac{\epsilon^2}{4}y^2}}{(1+\epsilon^2)^{5/2}}\Big(1+\frac{\epsilon^2}{2}\Big)\Big\{1+\frac{1+\frac{\epsilon^2}{2x_{\rm B}}}{1+\frac{\epsilon^2}{2}}\frac{x_{\rm B}t}{\mathcal{Q}^2}\Big\},\\
S_{0+}(n=1) &= -\frac{8\sqrt{2}(2-y)y\sqrt{1-y-\frac{\epsilon^2}{4}y^2}}{(1+\epsilon^2)^2}\frac{\tilde{K}^2}{\mathcal{Q}^2},\\
S_{0+}(n=2) &= -\frac{8\sqrt{2}Ky\sqrt{1-y-\frac{\epsilon^2}{4}y^2}}{(1+\epsilon^2)^2}\Big(1+\frac{\epsilon^2}{2}\Big)\Big\{1+\frac{1+\frac{\epsilon^2}{2x_{\rm B}}}{1+\frac{\epsilon^2}{2}}\frac{x_{\rm B}t}{\mathcal{Q}^2}\Big\}.
\end{aligned}
\tag{B2}
$$

Finally, the helicity-flip transverse-transverse coefficients are

$$
\begin{aligned}
C_{-+}(n=0) &= \frac{8(2-y)}{(1+\epsilon^2)^{3/2}}\Big\{(2-y)^2\frac{\sqrt{1+\epsilon^2}-1}{2(1+\epsilon^2)}\frac{\tilde{K}^2}{\mathcal{Q}^2}+\frac{1-y-\frac{\epsilon^2}{4}y^2}{\sqrt{1+\epsilon^2}}\Big(1-x_{\mathrm{B}}-\frac{\sqrt{1+\epsilon^2}-1}{2}+\frac{\epsilon^2}{2x_{\mathrm{B}}}\Big)\frac{x_{\mathrm{B}}tt'}{\mathcal{Q}^4}\Big\},\\
C_{-+}(n=1) &= \frac{8K}{(1+\epsilon^2)^{3/2}}\Big\{(2-y)^2\frac{2-\sqrt{1+\epsilon^2}}{1+\epsilon^2}\Big(\frac{\sqrt{1+\epsilon^2}-1+\epsilon^2}{2(2-\sqrt{1+\epsilon^2})}\Big(1-\frac{t}{\mathcal{Q}^2}\Big)-\frac{x_{\mathrm{B}}t}{\mathcal{Q}^2}\Big)\\
&\quad+2\frac{1-y-\frac{\epsilon^2}{4}y^2}{\sqrt{1+\epsilon^2}}\Big(\frac{1-\sqrt{1+\epsilon^2}+\frac{\epsilon^2}{2}}{2\sqrt{1+\epsilon^2}}+\frac{t}{\mathcal{Q}^2}\Big(1-\frac{3x_{\mathrm{B}}}{2}+\frac{x_{\mathrm{B}}+\frac{\epsilon^2}{2}}{2\sqrt{1+\epsilon^2}}\Big)\Big)\Big\},\\
C_{-+}(n=2) &= 4(2-y)\Big(1-y-\frac{\epsilon^2}{4}y^2\Big)\frac{1+\sqrt{1+\epsilon^2}}{(1+\epsilon^2)^{5/2}}\Big\{(2-3x_{\mathrm{B}})\frac{t}{\mathcal{Q}^2}+\Big(1-2x_{\mathrm{B}}+\frac{2(1-x_{\mathrm{B}})}{1+\sqrt{1+\epsilon^2}}\Big)\frac{x_{\mathrm{B}}t^2}{\mathcal{Q}^4}\\
&\quad+\Big(1+\frac{\sqrt{1+\epsilon^2}+x_{\mathrm{B}}+(1-x_{\mathrm{B}})\frac{t}{\mathcal{Q}^2}}{1+\sqrt{1+\epsilon^2}}\frac{t}{\mathcal{Q}^2}\Big)\epsilon^2\Big\},\\
C_{-+}(n=3) &= -8K\Big(1-y-\frac{\epsilon^2}{4}y^2\Big)\frac{1+\sqrt{1+\epsilon^2}+\frac{\epsilon^2}{2}}{(1+\epsilon^2)^{5/2}}\Big\{1+\frac{1+\sqrt{1+\epsilon^2}+\frac{\epsilon^2}{2x_{\mathrm{B}}}}{1+\sqrt{1+\epsilon^2}+\frac{\epsilon^2}{2}}\frac{x_{\mathrm{B}}t}{\mathcal{Q}^2}\Big\},\\
S_{-+}(n=1) &= -\frac{4K(2-y)y}{(1+\epsilon^2)^2}\Big\{1-\sqrt{1+\epsilon^2}+2\epsilon^2-2\Big(1+\frac{\sqrt{1+\epsilon^2}-1}{2x_{\mathrm{B}}}\Big)\frac{x_{\mathrm{B}}t}{\mathcal{Q}^2}\Big\},\\
S_{-+}(n=2) &= -2y\Big(1-y-\frac{\epsilon^2}{4}y^2\Big)\frac{1+\sqrt{1+\epsilon^2}}{(1+\epsilon^2)^2}\Big(\epsilon^2-2\Big(1+\frac{\epsilon^2}{2x_{\mathrm{B}}}\Big)\frac{x_{\mathrm{B}}t}{\mathcal{Q}^2}\Big)\Big\{1+\frac{\sqrt{1+\epsilon^2}-1+2x_{\mathrm{B}}}{1+\sqrt{1+\epsilon^2}}\frac{t}{\mathcal{Q}^2}\Big\}.
\end{aligned}
\tag{B3}
$$

[1] D. Müller, D. Robaschik, B. Geyer, F.-M. Dittes, and J. Horejsi, Fortschr. Phys. **42**, 101 (1994); X. Ji, Phys. Rev. D **55**, 7114 (1997); A. V. Radyushkin, Phys. Rev. D **56**, 5524 (1997).

[2] M. Burkardt, Phys. Rev. D **62**, 071503 (2000); **66**, 119903 (E) (2002); M. Diehl, Eur. Phys. J. C **25**, 223 (2002); **31**, 277(E) (2003); J. P. Ralston and B. Pire, Phys. Rev. D **66**, 111501 (2002); A. V. Belitsky and D. Müller, Nucl. Phys. A **711**, 118 (2002).

[3] A. V. Belitsky, X. Ji, and F. Yuan, Phys. Rev. D **69**, 074014 (2004).

[4] K. Goeke, M. V. Polyakov, and M. Vanderhaeghen, Prog. Part. Nucl. Phys. **47**, 401 (2001); M. Diehl, Phys. Rep. **388**, 41 (2003); A. V. Belitsky and A. V. Radyushkin, Phys. Rep. **418**, 1 (2005).

[5] I. V. Anikin, B. Pire, and O. V. Teryaev, Phys. Rev. D **62**, 071501 (2000).

[6] M. Penttinen, M. V. Polyakov, A. G. Shuvaev, and M. Strikman, Phys. Lett. B **491**, 96 (2000).

[7] A. V. Belitsky and D. Müller, Nucl. Phys. **B589**, 611 (2000).

[8] A. V. Radyushkin and C. Weiss, Phys. Lett. B **493**, 332 (2000); Phys. Rev. D **63**, 114012 (2001).

[9] N. Kivel, M. V. Polyakov, A. Schäfer, and O. V. Teryaev, Phys. Lett. B **497**, 73 (2001).

[10] A. V. Belitsky, D. Müller, and A. Kirchner, Nucl. Phys. **B629**, 323 (2002).

[11] A. Kirchner, and D. Mueller, Eur. Phys. J. C **32**, 347 (2003).

[12] P. Kroll, M. Schürmann, and P. A. M. Guichon, Nucl. Phys. A **598**, 435 (1996).

[13] M. Diehl, T. Gousset, B. Pire, and J. P. Ralston, Phys. Lett. B **411**, 193 (1997).

[14] A. V. Belitsky, D. Müller A. Kirchner, and A. Schäfer, Phys. Rev. D **64**, 116002 (2001).

[15] C. Itzykson and J. Zuber, *Quantum Field Theory* (McGraw-Hill, New York, 1980).

[16] A. V. Belitsky, D. Müller, L. Niedermeier, and A. Schäfer, Nucl. Phys. **B593**, 289 (2001).

[17] N. Kivel and L. Mankiewicz, Eur. Phys. J. C **21**, 621 (2001).

[18] R. K. Ellis, W. Furmanski, and R. Petronzio, Nucl. Phys. **B212**, 29 (1983).

[19] X. Ji and J. Osborne, Phys. Rev. D **57**, R1337 (1998); A. V. Belitsky and D. Müller, Phys. Lett. B **417**, 129 (1998); L. Mankiewicz, G. Piller, E. Stein, M. Vänttinen, and T. Weigl, Phys. Lett. B **425**, 186 (1998).

[20] D. Müller, Phys. Lett. B **634**, 227 (2006); K. Kumericki, D. Müller, K. Passek-Kumericki, and A. Schäfer, Phys. Lett. B **648**, 186 (2007); K. Kumericki, D. Müller, and K. Passek-Kumericki, Nucl. Phys. **B794**, 244 (2008).

[21] N. Kivel and L. Mankiewicz, Nucl. Phys. **B672**, 357 (2003).

[22] P. Hoodbhoy and X. Ji, Phys. Rev. D **58**, 054006 (1998).

[23] A. V. Belitsky and D. Müller, Phys. Lett. B **486**, 369 (2000).
[24] M. Diehl, Eur. Phys. J. C **19**, 485 (2001).
[25] A. V. Belitsky and D. Müller, Phys. Lett. B **507**, 173 (2001).
[26] A. V. Belitsky, A. Kirchner, D. Müller, and A. Schäfer, Phys. Lett. B **510**, 117 (2001).
[27] M. Vanderhaeghen, P. A. M. Guichon, and M. Guidal, Phys. Rev. D **60**, 094017 (1999).